EXPERIENCE WITH CBETA ONLINE MODELING TOOLS

C. Gulliford, D. Sagan, A. Bartnik, J. Dobbins, Cornell University, Ithaca, NY, USA

J. S. Berg, BNL, Upton, Long Island, New York, USA,

Antonett Nunez-delPrado, Department of Physics, University of Central Florida

Abstract

The Cornell-Brookhaven CBETA machine is a four pass Energy Recovery Linac (ERL) with a Non-scaling Fixed-Field Alternating gradient (NS-FFA) arc. For online modeling of single particle dynamics in CBETA, a customized version of the Tao program, which is based upon the Bmad toolkit, has been developed. This online program, called CBETA-V, is interfaced to CBETA's EPICS control system. This paper describes the online modeling system and initial experience during machine running.

INTRODUCTION

The Cornell-Brookhaven Energy recovery linac Test Accelerator (CBETA) [1], currently under construction at Cornell University, is a 4-pass, 150 MeV Energy Recovery Linac (ERL), utilizing a Non-Scaling Fixed Field Alternating-gradient (NS-FFA) permanent magnet return loop. CBETA is a joint collaboration of Brookhaven National Laboratory (BNL) and the Cornell Laboratory for Accelerator based Sciences and Education (CLASSE).

The CBETA project builds on the significant advancements in high-brightness photoelectron sources and Superconducting RF (SRF) technology developed at Cornell [2–5], as well as the FFA magnet and lattice design expertise from BNL. One aim of CBETA is to establish the operation of a multi-turn SRF based ERL utilizing a compact FFA return loop with large energy acceptance (a factor of roughly 3.6 in energy), and thus demonstrate the feasibility of one possible cost-reduction technology under consideration for the eRHIC Electron-Ion Collider (EIC) currently being designed at BNL. The CBETA project involves the study and measurement of many critical phenomena relevant to proposed EIC machine designs: the Beam-Breakup (BBU) instability, halo-development and collimation, growth in energy spread from Coherent Synchrotron Radiation (CSR), and CSR micro bunching. The CBETA project should provide valuable insight for both the EIC and ERL communities [1].

As part of the CBETA commissioning sequence, a combined test of the elements of all of the critical subsystems required for the CBETA project was done in the spring of 2018. This "Fractional Arc Test" (FAT) involved the injector, the Main Linac Cryomodule (MLC), the low energy splitter line, and a first prototype production permanent magnet girder featuring four cells of the FFA return loop (see Fig. 1). Besides hardware, the FAT commissioning involved testing and benchmarking of CEBTA-V, the CBETA online model. This paper describes the online modeling system and initial experience during machine running.

ONLINE SIMULATION ENVIRONMENT

The online single particle dynamics simulation model CBETA-V is based upon Bmad [6] and Tao [7]. Bmad is a modular, object-oriented subroutine library for simulating charged particle beams in high-energy accelerators and storage rings. Tao is a general purpose design and simulation program based upon Bmad and includes several optimization routines allowing the user to correct orbits, fit measured data, etc.

There were a number of advantages to basing CBETA-V on Bmad and Tao. For one, the majority of the CBETA lattice design was done using Bmad and Tao. This, and the fact that any Bmad based program is able to read Bmad lattice files, meant that offline and online simulations could be seamlessly interfaced. Additionally, the modular nature of both Bmad and Tao meant that CBETA-V development essentially consisted of creating a custom version of Tao which had the ability to communicate with the CBETA online EPICS database [8]. This was a relatively simple procedure requiring development of only about 1500 lines of code, and resulted in an online program which had all the capabilities of Tao. The ease of which CBETA-V was implemented is due in no small part to the fact that Bmad was originally developed for use with online modeling. Chan-
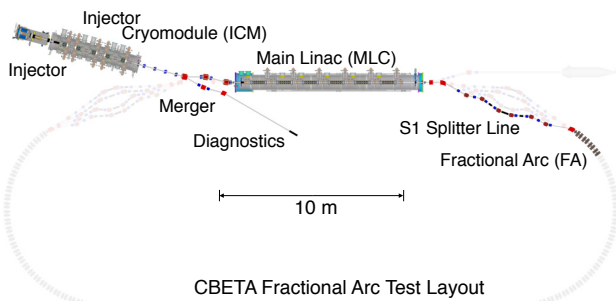

Figure 1: Schematic of the CBETA machine highlighting the components installed for Fractional Arc Test.
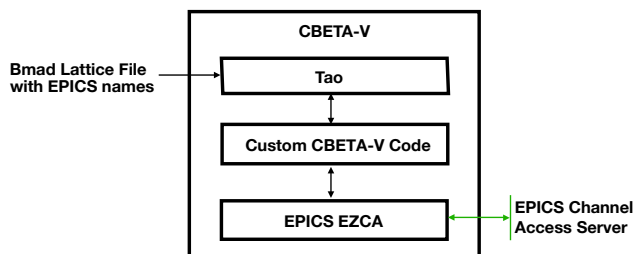

Figure 2: Schematic of the CBETA-V application showing the linking of the Tao with the EPICS EZCA library.
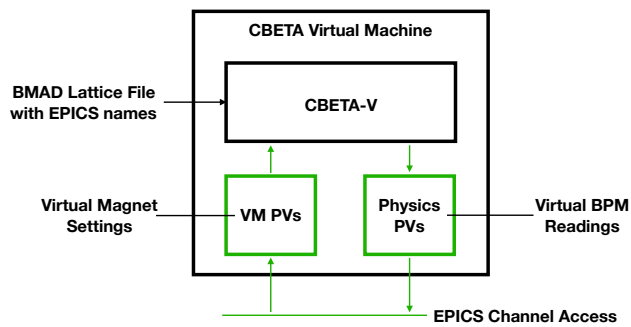
TUPAF10

Figure 3: Schematic of the CBETA Virtual Machine application showing the communication between an outside EPICS user and CBETA-V via the CBETA Virtual Machine "virtual" control system.

Figure 4: Real time comparison of an orbit bump. Circles indicate data read from the CBETA BPMs, while the blue line indicates the simulated values.

nel Access between CBETA-V and the EPICS database is achieved via the EZCA [8] C/Fortran interface library as illustrated in Fig. 2. Additionally, CBETA-V (and Tao) can be interfaced to Python using the Python foreign function library ctypes or the Python pexpect module. The Bmad lattice files for CBETA have EPICS Process Variable (PV) information attached to corresponding physical elements which allows CBETA-V to translate between EPICS PV values and the CBETA machine state. The calibration constants needed to convert machine readback quantities (such as magnet currents) into field strengths (such as quadrupole focusing strengths) are incorporated into the EPICS database so that CBETA-V works independently of any calibration constants.

In order to simulate space charge effects in the low energy part of CBETA, the General Particle Tracer (GPT) program [9] is used for simulations from the cathode through the first pass of the main linac. MATLAB was interfaced to GPT to facilitate communication between GPT and EPICS. Features of this MATLAB/GPT program include the ability to save and load optics settings and simulation results to and from a file, the ability to load injector settings from the machine and independently adjust them in simulation, as well as the ability to visualize all relevant simulation data [3].

Building on CBETA-V, a second application, called the CBETA Virtual Machine (CBETA-VM), was designed. This software creates its own copy of the CBETA EPICS control system, allowing users to command the virtual optical elements in the simulation via standard EPICS commands. Figure 3 shows a schematic of this application. By changing any of the element strengths in the model, the software computes all relevant single particle tracking parameters (that is, centroid orbit, dispersion, transfer matrix, etc), and publishes the results to its own EPICS records, thus making the virtual machine data available to the user via EPICS in exactly the same manner as real machine data. This allows for any automated measurement procedure to command and take data from either/both the real or virtual machine. This provides the ability to easily produce simulated predictions of measurement results, as well as the ability to realistically
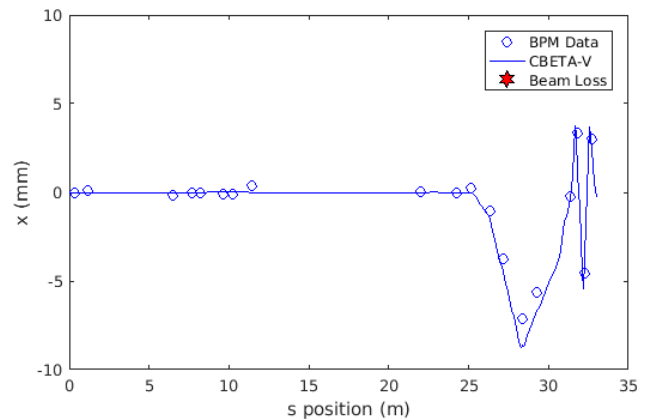
debug automated measurement procedures. Many of the experimental procedures used in CBETA were developed and tested offline in this manner. The software also provides a "sync" mode where the Virtual Machine continuously monitors the status of the real CBETA settings, and updates the simulated machine data upon detecting a change in the settings of the real machine, thus providing a useful online diagnostic.

REAL TIME COMPARISON WITH MEASUREMENTS

By serving simulated physics data from CBETA-V via EPICS records, the CBETA-VM enables any client application which can read EPICS PVs capable of accessing simulation data by reading the corresponding virtual EPICS records. For machine data that can be read out continuously, such as BPM data, this makes visual comparison of the measured and simulated data straightforward. Figure 4 shows an example snap shot of an orbit bump generated in the S1 splitter line. With CBETA-VM in sync mode, changing the S1 corrector responsible for the bump produced a simulated curve and measured data points that closely moved together.

In general, data (such as orbit data) from the real machine is limited to a finite number of locations throughout the machine. This makes the real time inclusion of simulated smooth data curves in the same displays as the real data useful as it "completes" the real data by filling in the values in between diagnostic points. In addition to this, once the accuracy of the CBETA-VM was established, it provided accurate simulated information for which there is no corresponding read out that is continuous in time. Quantities useful in operation include the beam energy, dispersion, BPM time of arrival through the FAT lattice, R_{56} transfer matrix element.

OFFLINE MEASUREMENT ANALYSIS

Some important quantities are not directly measured but must be calculated from direct measurements. For example, to measure the dispersion, the voltage of the last MLC cavity

(a)

(a)   Orbit response to the MS1DPB01 dipole.

(b)

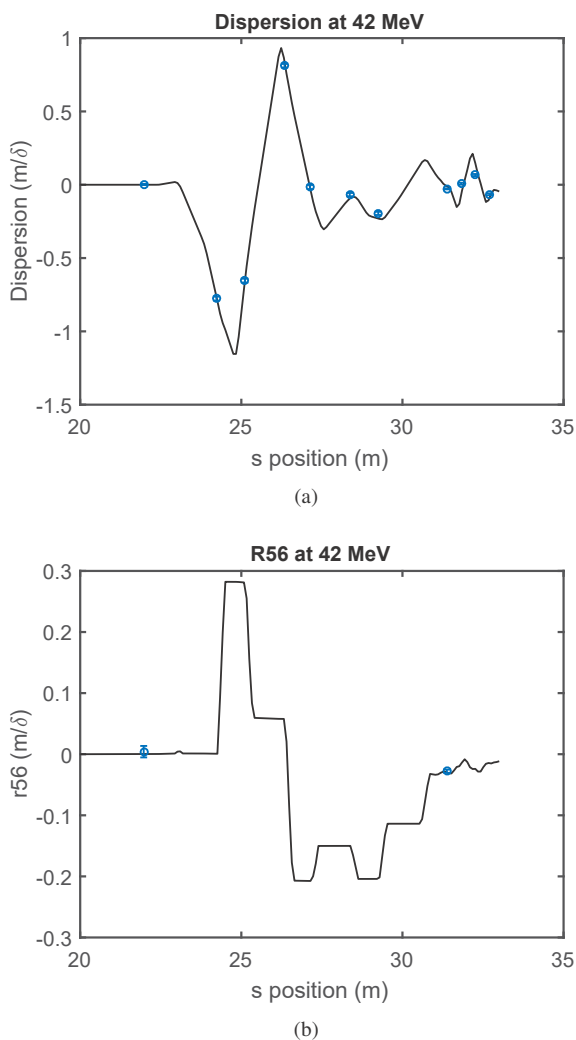(b)   Orbit response to the MS1CRV01 vertical corrector.

Figure 5: Comparison of the measured (blue circles) and simulated (black line) data. Measurements where made at the nominal 42 MeV energy. (a) Dispersion measurement, and (b) The time of arrival derivative with respect to energy, R_{56}. The two data points correspond to the first BPM after the MLC and the first FA BPM in the fractional arc.

was scanned and the resulting orbit position changes measured downstream. The dispersion was computed by fitting curves to the position changes on each BPM and extracting the linear variation around the nominal voltage set-point. Since such quantities as the dispersion require some amount of time to take data, the analysis essentially has to be done "offline".

Figure 5(a) shows measured dispersion data along with the simulated prediction at the nominal S1 energy of 42 MeV. In addition to recording the BPM positions downstream of the linac during the dispersion measurement, the procedure also saved the BPM time of arrival ϕ (in units of the RF phase) on the first BPM after the MLC as well as the first FA BPM in the fractional arc. This allows for the determination of the R_{56} matrix element through the splitter line. Figure 5(b) displays the resulting measured and simulated R_{56}, defined as $R_{56} = (c/\omega)d\phi/d\delta$ where δ denotes a relative
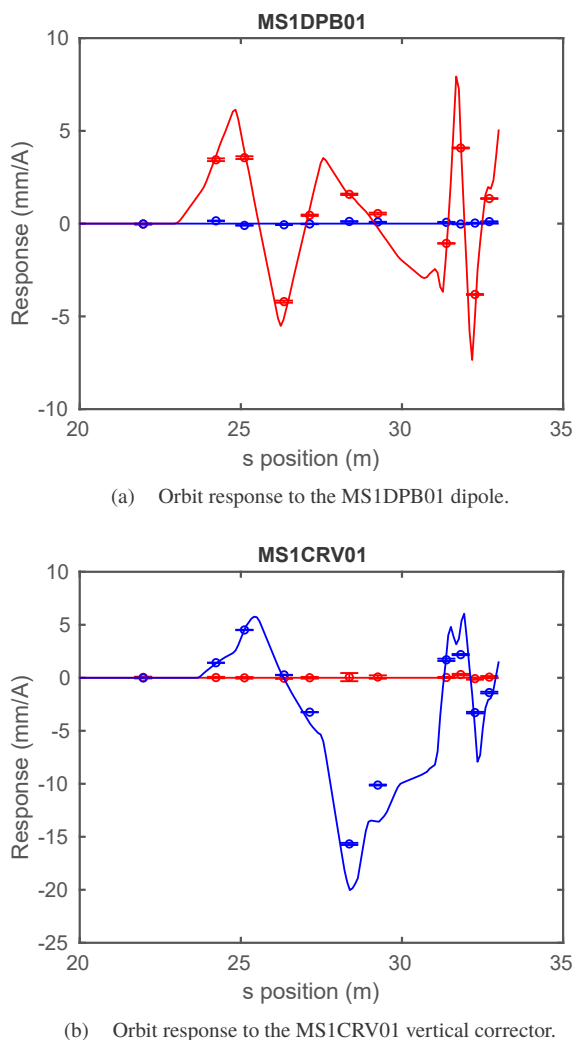
Figure 6: Measured orbit response (points) compared to simulation (lines). Horizontal response is shown in red, and vertical in blue. (a) Response to the variation of the first S1 splitter dipole. (b) Response to the variation of the first S1 splitter vertical corrector.

energy change. The excellent agreement between simulation and measurement seen in both the dispersion and R_{56} data required adjusting the simulated S1 quadrupole settings by 1%. Similar agreement were found for the comparison of the measured dispersion and R_{56} at beam energies ranging from 38.5 to 59 MeV.

In addition to the above results, the orbit response matrix was also measured during FAT commissioning. To do so, every corrector and dipole magnet in the machine was scanned and the resulting orbit position changes recorded. The slope of the fit of position verses magnet strength at the nominal magnet settings gives the response matrix. Figures 6(a) and 6(b) show the BPM response to the variation of two S1 magnets downstream of the MLC. The measured data and simulated responses agree well, especially for the horizontal orbit.

TESTING ORBIT CORRECTION PROCEDURES OFFLINE

Orbit correction studies for the CBETA machine up until FAT commissioning were carried out offline from the EPICS control system/real machine. Unfortunately, the tight schedule of the Fractional Arc Test did not allow for significant tests of orbit correction software during the experiment. Consequently, the CBETA-VM was used to perform virtual orbit correction experiments originally planned for during commissioning [10]. Orbit corrections were done using Singular Value Decomposition (SVD) since that technique had proved robust in the past.

One test involved the viability of orbit correction in the injector section following the ICM and before the MLC. The test proceeded as follows: first the orbit response matrix R is computed in the lattice model. Random errors to the quadrupole calibrations in the beamline were assigned by scaling the corresponding quadrupole currents using a 25% RMS normal distribution. In addition, random quadrupole offsets with an RMS spread of 1 mm in both the horizontal and vertical planes were introduced. Finally, the correctors in the sections of the machine between the ICM and MLC were randomly set in order to produce initial "uncorrected" orbits. Fig 7(a) shows 100 examples of these uncorrected orbits. In this plot (as well Fig. 7(b)), the red dots indicate BPM readings.

These orbits were then corrected using SVD, with a singular value tolerance of 0.4345 used for finding the pseudo-inverse of R. Because R was computed for the nominal machine state (on-axis orbit, no quadrupole scaling errors or misalignments), the correction algorithm was iterated 10 times. Figure 7(b) shows the resulting orbits which have been reduced in scale by a factor of roughly 100.

To further quantify the residual orbit, the RMS of the virtual BPM readings,

$$\sigma_{Res} = \sqrt{\frac{1}{2N}\sum_i (x_i^2 + y_i^2)}, \qquad (1)$$

after each iteration of the SVD procedure was calculated and shown in Fig. 8. Here i runs over all the BPMs in the FAT layout. From this we conclude that the SVD algorithm produces sub-micron residual orbit error within a few (roughly 3-4) iterations.

In addition to this test, the steering of the beam onto the periodic orbit in the FA section of the FAT layout was also solved using SVD. When the beam is steered onto the periodic orbit, the FA BPMs should read the same value horizontally (vertically the orbit should be zero). Before correction, denote the horizontal positions on the FA BPMs by **x**, and denote the desired periodic orbit by $\mathbf{C} = C \cdot (1, 1, ..., 1)^T$ where the constant C is the as yet unknown periodic offset. The matrix problem for finding the change in corrector currents $\Delta\mathbf{I}$ that will give periodic orbit readings can be written as:

$$\begin{pmatrix} R_{11} & R_{12} & \dots & R_{1N} & 1 \\ R_{21} & R_{22} & & R_{2N} & 1 \\ R_{31} & & & R_{3N} & 1 \\ \vdots & & & \vdots & \vdots \\ R_{M1} & & & R_{MN} & 1 \end{pmatrix} \begin{pmatrix} \Delta I_1 \\ \Delta I_2 \\ \vdots \\ \Delta I_N \\ -C \end{pmatrix} = - \begin{pmatrix} x_1 \\ x_2 \\ x_3 \\ \vdots \\ x_M \end{pmatrix} \qquad (2)$$

where the R_{ij} are the elements of the corrector to BPM response matrix R. Inverting this equation using SVD allows for the determination of both the corrector currents **I** and periodic BPM reading C simultaneously.

To test this, the response matrix from the last two dipole magnets in the S1 splitter line to the four BPMs in the FA section was computed, and the matrix in Eq. (2) formed. Using the fact that the periodic orbit solution in the FA section is a function of energy, ten non-periodic orbits were constructed by scanning the beam energy from 39 to 59 MeV (corresponding to the energy ranged demonstrated in the FAT). The SVD steering algorithm was then applied and iterated ten times at each energy. Figure 9(a) shows the ten different non-periodic initial orbits.

The results of the SVD operation are shown in Fig. 9(b) and show that the periodic orbit has been found. To get a sense of the level at which the orbit is periodic on the FA BPMs, the error in the periodicity of the orbit is defined as

$$\sigma_{Res} = \sqrt{\frac{1}{2N}\sum_{i,j}(x_i - x_j)^2}. \qquad (3)$$

where i and j run over the four BPMs in the FFA fractional arc. Clearly this quantity vanishes when the orbit is periodic. Figure 10 shows the residuals found as a function of SVD iteration for the ten example energies shown in Figs. 9(a) and 9(b). Note that for some of the energies in this example, the graph of the RMS orbit residual only extends to about three to five iterations. In these examples, applying SVD algorithm resulted in a perfectly periodic orbit and thus the RMS orbit residual is exactly zero (which is not shown on a log scale plot). As can be seen, the SVD technique works well in both examples and provides an important proof of principle for the online procedure.

CONCLUSION

The flexibility built into the Bmad toolkit and the Tao program allowed for the timely construction of both online and offline models for CBETA and results from the FAT experiment verified the rationality of the design approach as well as the usefulness of both the CBETA-V online model and virtual machine. The flexibility of the design allows modifications to be added as needed relatively simply.

With this in mind, work on including a single pass CBETA lattice into CBETA-V has begun which will allow for additional offline testing of more complicated orbit correction and steering algorithms using the CBETA-VM prior to the next beam commissioning period. In addition to this work, significant effort is under way to fully take advantage of the

Uncorrected

Current Correction (N=8)
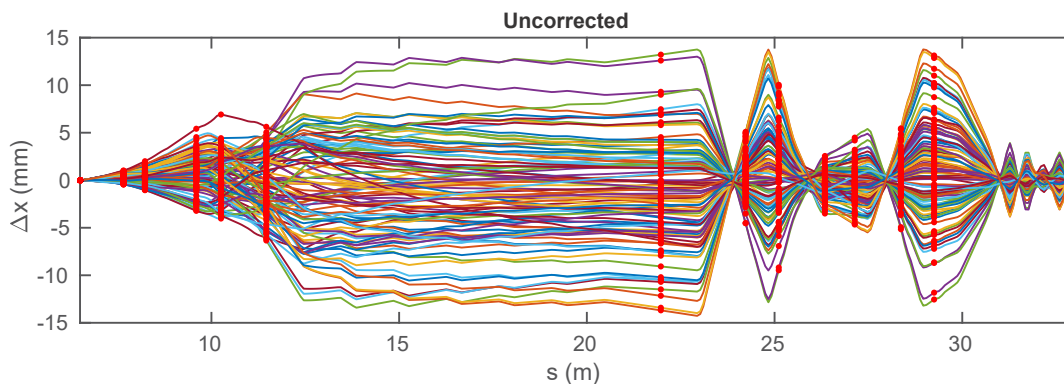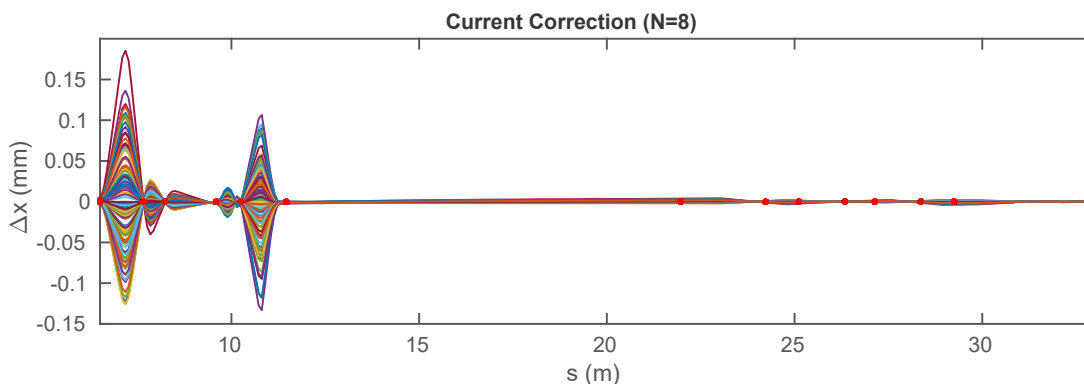
Figure 7: (a) Uncorrected orbits and (b) SVD corrected orbits. The red dots indicate BPM position/readings.
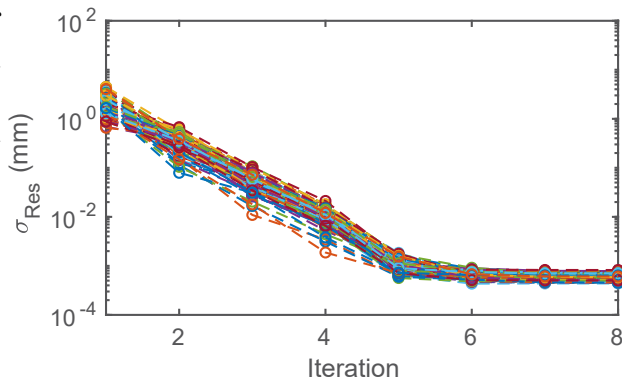
Figure 8: Correction error of the 100 simulated orbits as a function of SVD iteration.

flexibility of the Python language in restructuring the virtual machine wrapper. The purpose of this future work is to generalize and modularize the virtual machine layer so that users can add new physics tasks to the software at runtime, as well as allowing users to plug in different accelerator physics codes. Tests are underway of the latest version, with the hopes of this being ready for the next CBETA commissioning period as well.

ACKNOWLEDGEMENT

REFERENCES

[1] G. H. Hoffstaetter, *et al.*, *CBETA Design Report*, Cornell-BNL ERL Test Accelerator, ArXiv e-prints, June 2017.

[2] B. Dunham, *et al.*, "Record High-average Current from a High-brightness Photoinjector", *Applied Physics Letters*, vol. 102, no. 3, pp. 034105, 2013.

[3] C. Gulliford, *et al.*, "Demonstration of Low Emittance in the Cornell Energy Recovery Linac Injector Prototype", *Phys. Rev. ST Accel. Beams*, vol. 16, pp. 073401, July 2013.

[4] C. Gulliford, *et al.*, "Demonstration of cathode emittance dominated high bunch chargebeams in a DC gun-based photoinjector", *Applied Physics Letters*, vol. 106, no. 9, pp. 094101, 2015.

[5] R. Eichhorn, *et al.*, "The Cornell Main Linac Cryomodule: A Full Scale, High Q Accelerator Module for CW Application", *Physics Procedia*, vol. 67, pg. 785–790 , 2015.

[6] D. Sagan, "Bmad: A relativistic charged particle simulation", *Nuc. Instrum. Methods Phys. Res. A*, vol. 558, pp 356-59, 2006.

[7] D. Sagan and J. C. Smith, "The Tao Accelerator Simulation Program", in *Proc. PAC'05*, pg. 4159-–4161, May 2005.

[8] epics.anl.gov/extensions/ezca/index.php

[9] www.pulsar.nl/gpt/

[10] A. Nunez-delPrado and C. Gulliford, *CBETA-V: Advanced Online Simulation Tools for the CBETA Machine*, Cornell Internal Report, 2018.
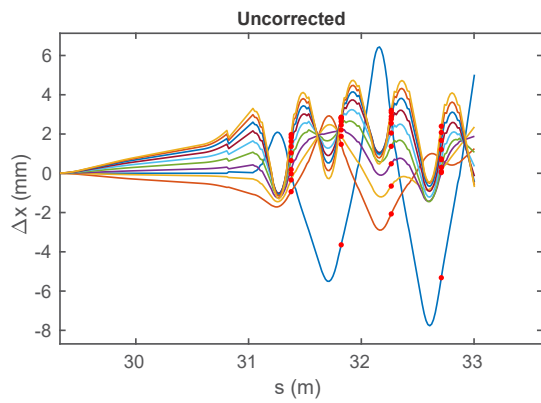
(a)   Horizontal orbit before SVD.
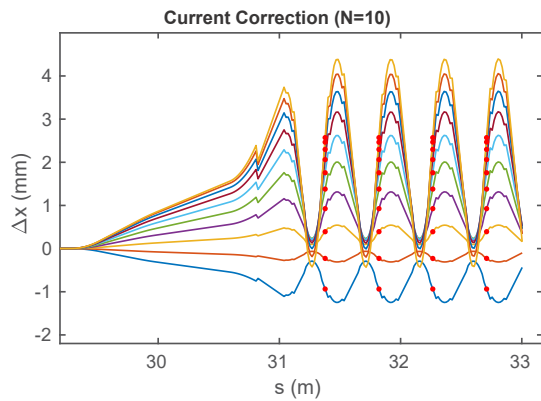
(b)   Horizontal orbit after SVD.

Figure 9: Steering onto the periodic orbit using SVD: (a) shows the initial non-periodic orbit for ten different beam energies, (b) shows the results of steering onto the period orbit using the last two dipoles in the splitter S1 section. The red circles indicate the BPM position and readout values.
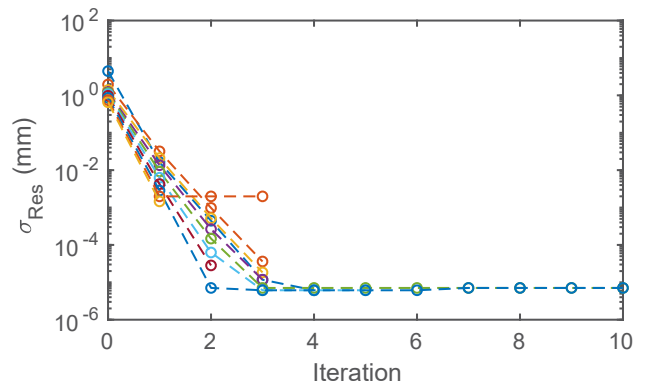

Figure 10: Correction error of the 10 simulated orbits with energies ranging from 39 to 52 MeV, as a function of the number of iterations of orbit correction.